Geochemical Perspectives Letters

Plume-lithosphere interaction, and the formation of fibrous diamonds

M.W. Broadley, H. Kagi, R. Burgess, D. Zedgenizov, S. Mikhail, M. Almayrac, A. Ragozin, B. Pomazansky, H. Sumino

Supplementary Information

The Supplementary Information includes:

- Samples and Geological Background
- Diamond FTIR and Nitrogen Aggregation
- Noble Gas Analysis
- Halogen Analysis
- Figures S-1 to S-5
- Tables S-1 and S-2
- Supplementary Information References

Sample and Geological Background

The Nyurbinskaya kimberlite pipe was discovered in 1994 in the Nakynsky kimberlite field, Yakutia (Spetsius *et al*., 2008). The kimberlite is one of the richest high-grade diamond deposit in Yakutia. The kimberlite was erupted 364 Ma and is similar in age to other Siberian diamond bearing kimberlites including: Mir, Internatsional'naya and Udachnaya (Davies *et al*., 1980; Kinny *et al*., 1997). Nyurbinskaya differs from other Yakutian kimberlites in its low Light Rare Earth Elements (LREE), Nb, Ta, U and Th contents (Agashev *et al*., 2001), it has therefore been classified as having a transitional composition between group I and II kimberlite types.

Mantle xenoliths from Nyurbinskaya are predominantly eclogitic, with only minor amounts of peridotites (Riches *et al*., 2010). The majority of diamonds originating from Nyurbinskaya can be classified into either those containing inclusions of eclogite minerals, or fibrous diamonds (Spetsius *et al*., 2017). The fibrous diamonds can be further subdivided in to three groups: coated, cloudy and cubic (Figure S-1). Coated diamonds, with green or yellow fibrous coats make up the majority of the fibrous diamonds, with cubic and cloudy diamonds being rarer (Spetsius *et al*., 2017).

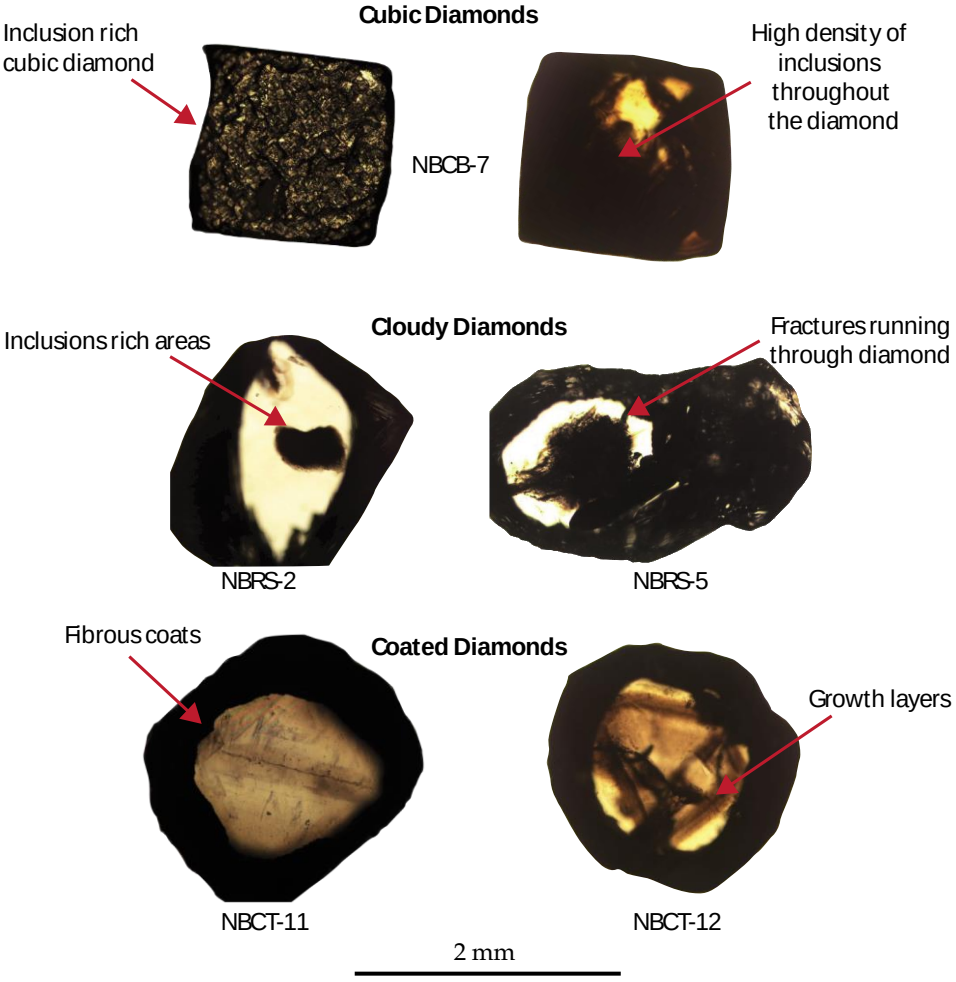

Figure S-1 Photomicrograph images of double cut and polished cubic, coated and cloudy diamonds from the Nyurbinskaya kimberlite. Cubic diamonds have a high density of fluid inclusions often rendering then completely opaque. The cloudy diamonds have internal areas rich in fluid inclusions whilst the majority of the fluid inclusions are within the fibrous coats of the coated diamonds. Note that diamond NBCT-12 was only analysed for nitrogen using FTIR and not for halogens and noble gases.

Diamond FTIR and Nitrogen Aggregation

Infrared absorption spectra were obtained for 29 diamonds using a Fourier transform infrared spectrometer (Spectrum 2000; Perkin Elmer Inc.) equipped with an IR microscope at Geochemical Research Center, The University of Tokyo. Samples were first mounted in indium and then analysed using a combination of a Globar light source, liquid nitrogen cooled MCT detector, and KBr beam splitter operating at a spectral resolution of 4 cm^{-1}. Spectral deconvolution was performed using the Diamap freeware (Howell *et al.*, 2012). Seven H_2O-rich samples (Fig. S-2) were then chosen for halogen and noble gas analysis.

Nitrogen is the most common impurity in natural diamonds. It is a relatively mobile element within the diamond lattice at mantle pressure and temperatures and as a result nitrogen defects in diamonds can evolve through time, which can be determined by FTIR. Nitrogen defects begin as single nitrogen atoms (C centres, Type Ib), which then evolves to pairs of nitrogen atoms (A centres, Type IaA), and finally to 4 nitrogen atoms tetrahedrally arranged about a vacancy (B centres, Type IaB). This evolution of N defect distribution through time is referred to as nitrogen aggregation (Evans and Qi, 1982). The evolution from C to A centre aggregation occurs rapidly (<1 Ma), while the evolution from A to B centres occurs much more slowly (over Ga). A to B centre aggregation follows a second-order kinetics law (Chrenko *et al.*, 1977), indicating it can be used to estimate either the mantle residence time of the diamond, or the average temperature at which it resided (assuming the other is known).

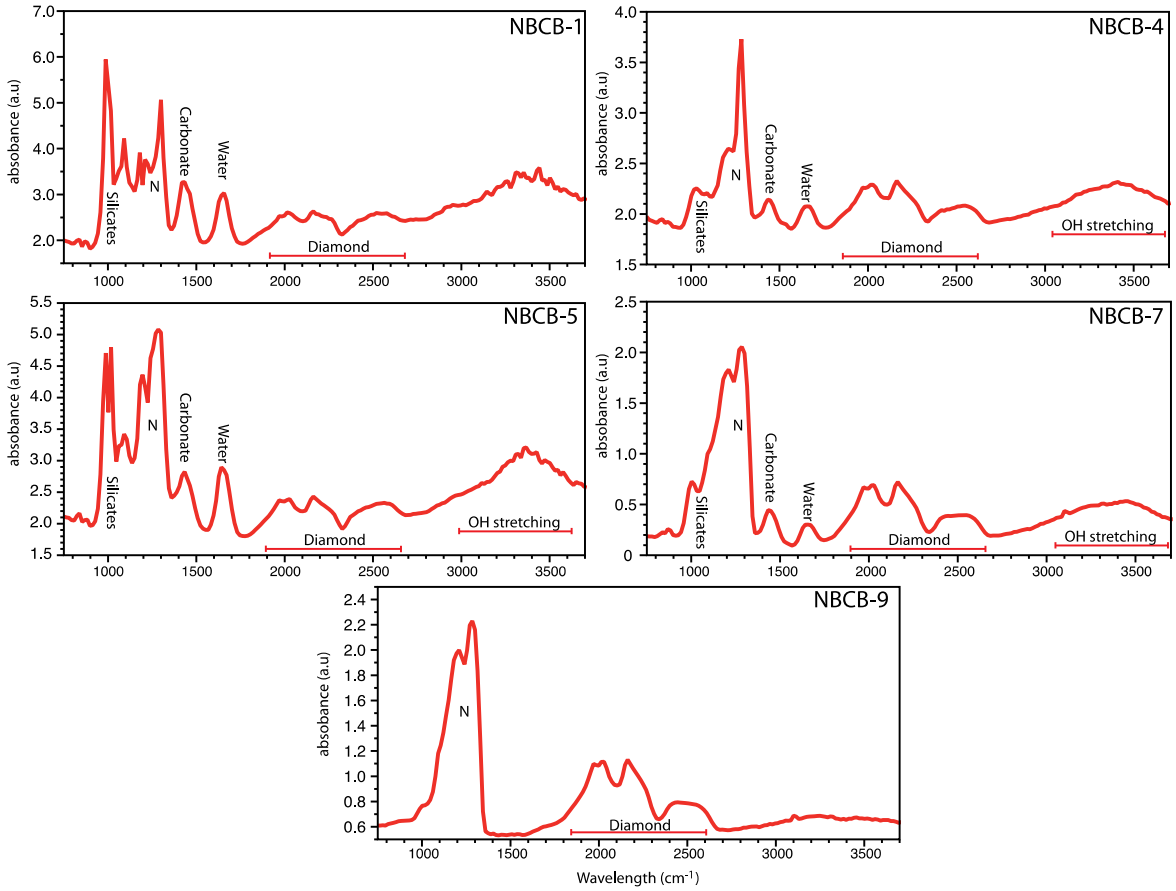

Figure S-2 FTIR spectra for all the cubic diamonds (NBCB) selected for noble gases and halogen analysis. Peaks representing hydrogen, water, silicates, carbonate and the range of OH stretching are all highlighted. All diamonds show evidence of being rich in a fluid component. Diamonds NBCB-1 and NBCB-5 have a poorly defined spectra due to the high density of fluid inclusions and opaque nature.

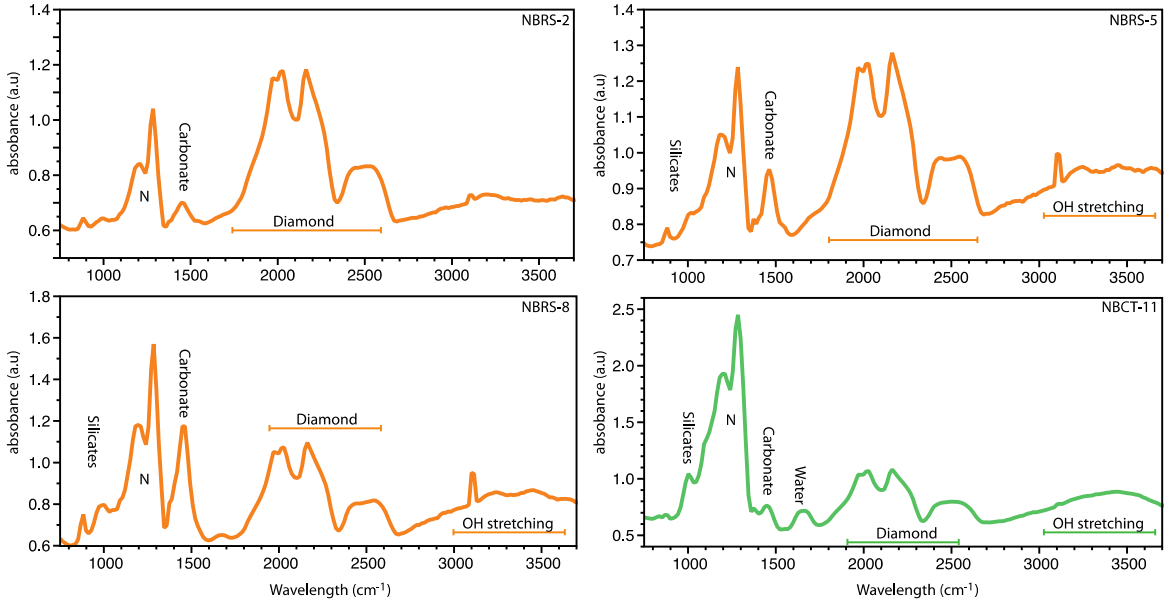

Figure S-3 FTIR spectra for all the cloudy (NBRS) and coated (NBCT) diamond selected for noble gases and halogen analysis. Peaks representing hydrogen, water, silicates, carbonate and the range of OH stretching are all highlighted. All diamonds show evidence of being rich in a fluid component.

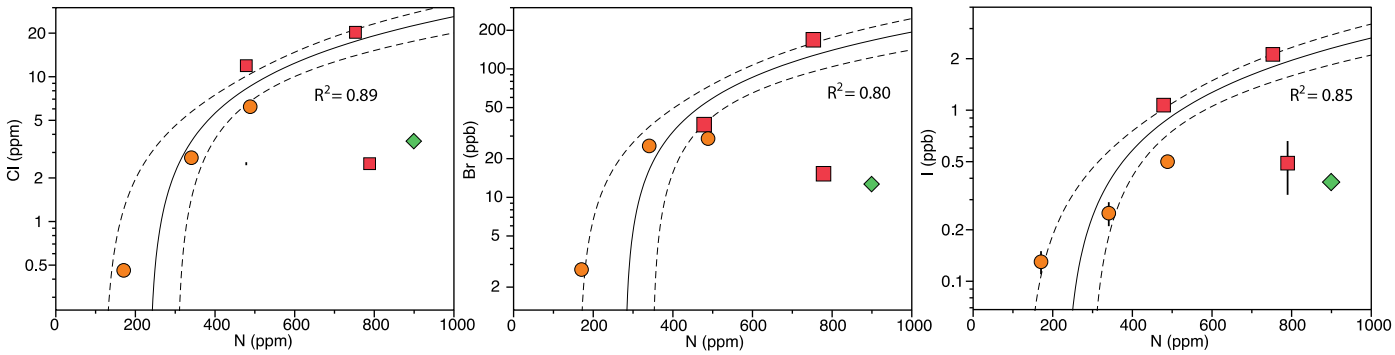

Figure S-4 Halogen concentrations *vs*. bulk nitrogen concentration. The concentration of Cl, Br and I of the cubic and cloudy diamonds are correlated with N concentrations. Black line represents a best fit of the cubic and cloudy diamonds data (excluding NBCB-4), with a 1σ uncertainty prediction (dashed lines). Coated diamond NBCT-11 and one cubic diamond (NBCB-4) do not fit along the same correlation line, suggesting that the halogens and N within the these diamonds may be related to another source, in agreement with the potentially higher mantle residence times (Fig. 4, main text). No evidence of correlation between N and noble gas concentrations exists suggesting that N and halogens may be more closely related to the trapped fluid inclusions, than the noble gases. All uncertainties are shown to 1σ. This correlation could be explained by nitrogen being present in the fluid as ammonic nitrogen, and so could form salt complexes with halogens, and therefore follow similar geochemical pathways. This inference is consistent with the predicted speciation of aqueous nitrogen at 5 GPa and up to 1000 °C in equilibrium with peridotitic and/or metasedimentary (eclogitic) mineral phases (Mikhail *et al*., 2017).

Noble Gas Analysis

Noble gases were first extracted from the diamonds *via* crushing. Individual diamonds were placed into a stainless steel crushing chamber, a steel ram attached to a bellows was then placed on top and the whole crusher was baked at 200 °C overnight under vacuum. The diamonds were then fractured by applying a hydraulic pressure (up to 70 MPa) to the steel ram using an external hydraulic hand pump. Extracted gases were purified by a series of Ti-Zr getters and then separated according to mass using a cryogenically cooled trap containing sintered-stainless steel. Helium, neon and argon were then released individually into the modified VG5400 mass spectrometer at the University of Tokyo for analysis following the procedure described in Sumino *et al*. (2001).

Roughly half of the crushed diamond chips were then analysed for He and Ne by bulk heating at the noble gas laboratory at CRPG, Nancy (France), using the Thermo Fischer Helix MC Plus. Samples weighing ~1-6 mg were loaded in an infrared laser chamber. The samples were pumped under high vacuum and baked at 110°C overnight to release any adsorbed atmospheric gases. Prior to analysis, blanks were measured to ensure the background of noble gases was low. Average blank values were 1.4 x 10^{-17} cm^3 STP ^{4}He and 1.5 x 10^{-15} cm^3 STP ^{20}Ne. The sensitivity and mass discrimination of the mass spectrometer was calibrated by the analysis of daily standards consisting of an atmospheric Ne standard and the HESJ standard for He, with has a ^{3}He/^{4}He ratio of 20.63 ± 0.10 R_A, where R_A is the ratio of atmosphere (Matsuda *et al*., 2002).

Gases were extracted from the diamonds using a CO_2 infrared (λ = 10.3 μm) laser for 5 minutes or until the diamonds were visibly graphitised. Noble gases were then first passed through an in-line Ti-sponge getter heated at 600 °C and purified with two Ti-sponge getters at 550 °C for 5 min. Argon was separated from He and Ne using a charcoal cold finger held at N_2 liquid temperature for 10 minutes and wasn't analysed in this study. Helium and neon were trapped using a cryogenic trap at 15K for 15 min. Helium was released at 34 K before being admitted to and analysed on the mass spectrometer. Neon was subsequently released at 110K and purified with a further two Ti-sponge getters, one at 550 °C and the other at the room temperature (~ 20 °C), for 10 minutes before analysis. The mass resolution of the MC Plus (~ 1800) enables the discrimination of the ^{20}Ne peak from $^{40}Ar^{++}$. Neon isotopes ratios were corrected for interference from CO_2^{++} with ^{22}Ne.

Differences between crushing and laser noble gas extraction

The maximum ^{40}Ar/^{36}Ar released from the cloudy and coated diamonds during crushing (461 ± 24) are closer to the atmospheric value of 298.6 (Lee *et al*., 2006), compared to cubic diamonds showing an average ^{40}Ar/^{36}Ar =1479 (Table S-2). The higher proportion of microinclusions in the cubic diamonds resulted in higher quantities of trapped noble gases released during crushing. The ^{40}Ar/^{36}Ar values of Ar released by laser heating of coated and cloudy diamonds (halogen analysis) are consistently higher (>1000) than the crushing release, whilst the cubic diamonds show little variation between crushing and heating. The difference in noble gas composition is considered to reflect the much higher abundance of microinclusions in cubic diamond coats and potential

release from the clear diamond sections of the cloudy and cubic diamonds during laser heating.

Concentrations of He are significantly lower during laser extraction compared to crushing, whilst Ne concentrations are similar during both extraction methods. Helium therefore appears to be more concentrated within the fluid inclusions relative to the diamond matrix. During graphitisation the majority of noble gases in the remaining fluid inclusion and the diamond matrix should be released. The low He and Ne concentrations during laser extraction suggest that the noble gas extraction was not completely efficient, possibly because of the build-up graphite on the sample surface impeding further release from deeper within the diamond. Despite the differences in He and Ne concentrations between the crushing and laser extraction the isotopic ratios are similar between the different extraction methods indicating the same volatile component is present in both the fluid and matrix phase of the diamonds.

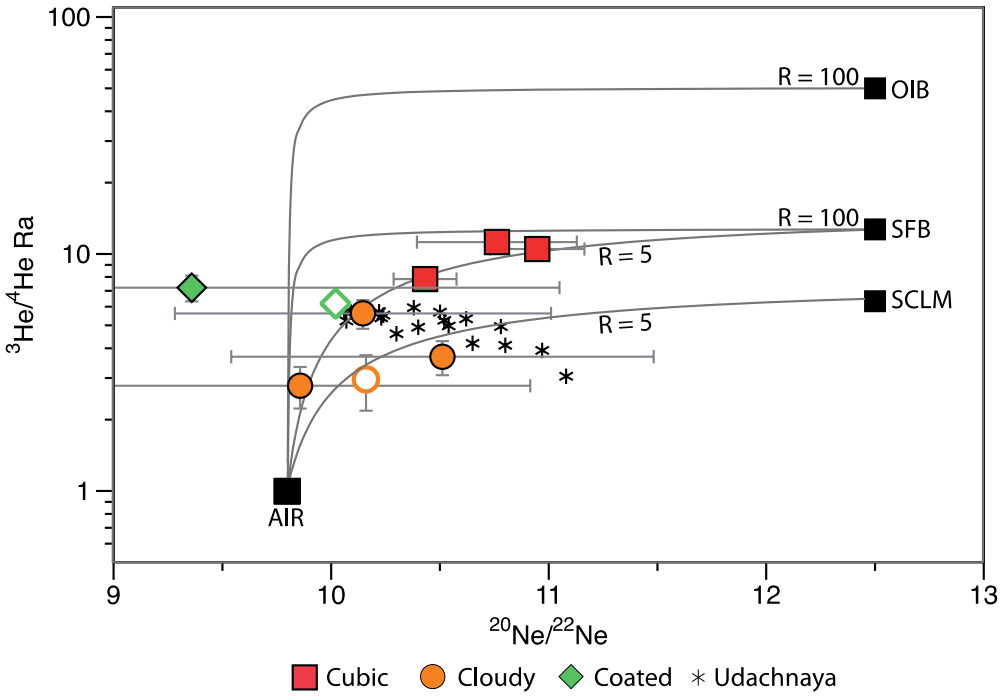

Figure S-5 $^3He/^4He$ *vs.* $^{20}Ne/^{22}Ne$ for Nyurbinskaya diamonds. The diamonds show a relationship between He and Ne and trend from air towards the value of the Siberian flood basalts (Basu *et al.*, 1995). There is potentially a third component present from the SCLM (having lower $^3He/^4He$ composition) that causes the mixing line to be shallower (R = 5) than generally expected for mixing between air and mantle alone (R = 100). Data for Udachnaya xenoliths are shown for reference indicating they contain a greater proportion of radiogenic ^4He from the SCLM relative to the Nyurbinskaya diamonds (Sumino *et al.*, 2006). Reference data for SCLM, MORB and OIB are from Gautheron and Moreira (2002); Graham (2002) and Stuart *et al.* (2003), respectively.

Halogen Analysis

The other half of the crushed diamond chips were analysed for their halogen abundance using Neutron-Irradiated Noble Gas Mass Spectrometry (NI-NGMS) at the University of Manchester following the methods outlined in Ruzié-Hamilton *et al.* (2016). Samples were weighed, wrapped in Al foil and vacuum encapsulated in a silica tube. Irradiation was carried out at for 24 hrs at the Safari-1 reactor, Pelindaba, South Africa (irradiation designated MN2017a). Noble gas proxy isotopes ($^{38}Ar_{Cl}$, $^{80}Kr_{Br}$, $^{128}Xe_{I}$ and $^{39}Ar_{K}$) formed during irradiation were measured on a Thermo Fisher Scientific ARGUS VI mass spectrometer. Prior to analysis, samples were baked at 150°C overnight to remove surficial adsorbed noble gases either from atmospheric contamination or from halogen producing noble gases during irradiation. Noble gases were released from the samples using a 10.6 μm wavelength CO2 laser. Halogens abundances were then calculated using well-defined conversion standards with known halogen concentrations (Hb3gr, scapolite and Shallowater meteorite), which monitor the efficiency of noble gas production through thermal and epithermal neutron reactions (Kendrick, 2012; Ruzié-Hamilton *et al.*, 2016).

Supplementary Tables

Table S-1 Halogen and nitrogen (bulk FTIR) concentrations and molar ratios as well as $^{40}Ar/^{36}Ar$ of Nyurbinskaya fibrous diamonds measured during neutron irradiation mass spectrometry. Sample NBCB-7 was lost during the irradiation process and therefore halogens were not measured within this sample. All uncertainties are 1σ

Sample	Mass (mg)	Cl (ppm)	±	Br (ppb)	±	I (ppb)	±	Br/Cl x 10^{-4}	±	I/Cl x 10^{-6}	±	$^{40}Ar/^{36}Ar$	±	N (ppm)
NBCB-1	3.1	11.92	0.44	36.82	3.52	1.07	0.09	13.71	1.26	14.59	1.44	1080.7	39.7	478
NBCB-4	0.6	2.51	0.06	15.27	1.34	0.49	0.05	26.98	2.38	31.80	3.95	529.5	35.1	782
NBCB-5	0.4	20.26	0.61	168.58	6.77	2.12	0.17	36.92	1.38	16.99	1.61	1667.9	94	753
NBRS-2	2.9	0.46	0.01	2.74	0.20	0.13	0.01	26.24	2.03	43.86	4.62	456.8	71.1	171
NBRS-5	1.9	2.76	0.05	25.14	0.85	0.25	0.02	40.38	1.54	14.74	1.44	1316.4	154.6	341
NBRS-8	1.5	6.21	0.12	28.67	1.37	0.50	0.04	20.49	1.04	13.00	1.29	2633.3	159.3	488
NBCT-11	2.6	3.59	0.07	12.68	0.55	0.38	0.03	15.68	0.74	17.26	1.64	2211.8	97.5	899

Table S-2 Helium and Neon concentration and isotopic ratios from crushing and laser extraction (italics) from the Nyurbinskaya diamonds. Diamond NBCB-9, was not successfully crushed and the complete diamond was analysed by laser extraction for noble gases. All uncertainties are reported to 1σ. n.d = not determined

Sample	Mass (mg)	^{4}He cm^{3} STP/g	±	$^{3}He/^{4}He$ R_A	±	^{20}Ne cm^{3} STP/g	±	$^{20}Ne/^{22}Ne$	±	$^{21}Ne/^{22}Ne$	±	$^{40}Ar/^{36}Ar$	±
NBCB-1	6.9	2.1×10^{-6}	8.5×10^{-8}	7.84	0.56	3.4×10^{-11}	3.7×10^{-12}	n.d	n.d	n.d	n.d	2755.7	198.1
	4.3	*n.d*	*n.d*	*n.d*	*n.d*	*1.6×10^{-10}*	*4.7×10^{-13}*	*10.04*	*0.04*	*0.031*	*0.0014*	*n.d*	*n.d*
NBCB-4	3.8	1.6×10^{-5}	6.9×10^{-7}	10.5	0.69	1.3×10^{-11}	6.4×10^{-11}	10.34	0.73	0.032	0.0029	862.5	61.8
NBCB-5	6.0	1.3×10^{-6}	5.9×10^{-7}	11.23	0.74	5.1×10^{-10}	2.7×10^{-11}	10.92	0.86	0.037	0.0039	1956.9	122.0
NBCB-9	*5.0*	*n.d*	*n.d*	*n.d*	*n.d*	*3.4×10^{-10}*	*9.0×10^{-13}*	*9.99*	*0.02*	*0.029*	*0.0005*	*n.d*	*n.d*
NBCB-7	5.8	2.3×10^{-6}	1.2×10^{-7}	9.95	0.77	3.6×10^{-10}	1.9×10^{-11}	10.76	0.88	0.032	0.0043	352.1	25.2
NBRS-2	7.3	2.4×10^{-7}	1.2×10^{-8}	3.65	0.78	1.8×10^{-10}	9.6×10^{-12}	10.15	0.86	0.029	0.0053	298.6	21.4
	3.8	*4.3×10^{-11}*	*9.3×10^{-12}*	*7.26*	*2.27*	*n.d*	*n.d*	*n.d*	*n.d*	*n.d*	*n.d*	*n.d*	*n.d*
NBRS-5	5.1	7.5×10^{-7}	3.8×10^{-8}	4.72	0.56	2.1×10^{-10}	1.2×10^{-11}	10.51	0.97	0.029	0.0070	437.6	31.4
	3.0	*2.2×10^{-9}*	*7.7×10^{-11}*	*2.96*	*0.95*	*3.2×10^{-11}*	*1.1×10^{-13}*	*10.16*	*0.04*	*0.030*	*0.0013*	*n.d*	*n.d*
NBRS-8	7.1	1.7×10^{-6}	7.2×10^{-8}	8.62	0.6	1.7×10^{-10}	1.1×10^{-11}	9.86	1.06	0.032	0.0077	461.0	24.0
	4.5	*9.8×10^{-10}*	*3.2×10^{-11}*	*5.62*	*0.37*	*n.d*	*n.d*	*n.d*	*n.d*	*n.d*	*n.d*	*n.d*	*n.d*
NBCT-11	6.3	4.0×10^{-7}	2.1×10^{-8}	7.21	0.9	5.8×10^{-11}	3.8×10^{-12}	9.36	1.69	0.033	0.0139	339.1	24.2
	3.4	*3.9×10^{-9}*	*3.1×10^{-11}*	*6.18*	*0.22*	*4.0×10^{-11}*	*1.4×10^{-13}*	*10.02*	*0.03*	*0.030*	*0.0005*	*n.d*	*n.d*

Supplementary Information References

Agashev, A.M., Watanabe, T., Bydaev, D.A., Pokhilenko, N.P., Fomin, A.S., Maehara, K., Maeda, J. (2001) Geochemistry of kimberlites from the Nakyn field, Siberia: evidence for unique source composition. *Geology* 29, 267-270.

Basu, A.R., Poreda, R.J., Renne, P.R., Teichmann, F., Vasiliev, Y.R., Sobolev, N.V., Turrin, B.D. (1995) High-3He plume origin and temporal-spatial evolution of the Siberian flood basalts. *Science* 269, 822-825.

Chrenko, R.M., Tuft, R.E., Strong, H.M. (1977) Transformation of the state of nitrogen in diamond. *Nature* 270, 141.

Davies, G., Sobolev, N.V., Khar'kiv, A.D. (1980) New data on the age of Yakutian kimberlites, obtained by U–Pb zircon dating. *Doklady Akademii Nauk SSSR* 254-1, 175–179.

Evans, T., Zengdu, Q. I. (1982) The kinetics of the aggregation of nitrogen atoms in diamond. *Proceedings of the Royal Society of London A* 381, 159-178.

Gautheron, C., Moreira, M. (2002) Helium signature of the subcontinental lithospheric mantle. *Earth and Planetary Science Letters* 199, 39-47.

Graham, D.W. (2002) Noble gas isotope geochemistry of mid-ocean ridge and ocean island basalts: Characterization of mantle source reservoirs. *Reviews in Mineralogy and Geochemistry* 47, 247-317.

Howell, D., O'Neill, C.J., Grant, K.J., Griffin, W.L., Pearson, N.J., O'Reilly, S.Y. (2012) μ-FTIR mapping: distribution of impurities in different types of diamond growth. *Diamond and Related Materials* 29, 29-36.

Kendrick, M.A. (2012) High precision Cl, Br and I determinations in mineral standards using the noble gas method. *Chemical Geology* 292, 116-126.

Kinny, P.D., Griffin, B.J., Heaman, L.M., Brakhfogel, F.F., Spetsius, Z.V. (1997) SHRIMP U-Pb ages of perovskite from Yakutian Kimberlites. apparent ages from Kimberlite derived low temperature garnet peridotites from Yakutia. *Proceedings of 6th International Kimberlite Conference, Novosibirsk, Russia*, 91-99.

Lee, J.Y., Marti, K., Severinghaus, J.P., Kawamura, K., Yoo, H.S., Lee, J.B., Kim, J.S. (2006) A redetermination of the isotopic abundances of atmospheric Ar. *Geochimica et Cosmochimica Acta* 70, 4507-4512.

Matsuda, J., Matsumoto, T., Sumino, H., Nagao, K., Yamamoto, J., Miura, Y., Kaneoka, I., Takahata, N., Sano, Y. (2002) The $^{3}He/^{4}He$ ratio of the new internal He Standard of Japan (HESJ). *Geochemical Journal* 36, 191-195.

Mikhail, S., Barry, P.H., Sverjensky, D.A. (2017) The relationship between mantle pH and the deep nitrogen cycle. *Geochimica Cosmochimica et Acta* 209, 149–160.

Spetsius, Z.V., Taylor, L.A., Valley, J.W., Deangelis, M.T., Spicuzza, M., Ivanov, A.S., Banzeruk, V.I. (2008) Diamondiferous xenoliths from crustal subduction: garnet oxygen isotopes from the Nyurbinskaya pipe, Yakutia. *European Journal of Mineralogy* 20, 375-385.

Spetsius, Z.V., Cliff, J., Griffin, W.L., O'Reilly, S.Y. (2017) Carbon isotopes of eclogite-hosted diamonds from the Nyurbinskaya kimberlite pipe, Yakutia: The metasomatic origin of diamonds. *Chemical Geology* 455, 131-147.

Sumino, H., Nagao, K., Notsu, K. (2001) Highly sensitive and precise measurement of helium isotopes using a mass spectrometer with double collector system. *Journal of the Mass Spectrometry Society of Japan* 49, 61-68.

Riches, A.J., Liu, Y., Day, J.M., Spetsius, Z.V., Taylor, L.A. (2010) Subducted oceanic crust as diamond hosts revealed by garnets of mantle xenoliths from Nyurbinskaya, Siberia. *Lithos* 120, 368-378.

Ruzié-Hamilton, L., Clay, P.L., Burgess, R., Joachim, B., Ballentine, C.J., Turner, G. (2016) Determination of halogen abundances in terrestrial and extraterrestrial samples by the analysis of noble gases produced by neutron irradiation. Chemical Geology, 437, 77-87.

Stuart, F.M., Lass-Evans, S., Fitton, J.G., Ellam, R.M. (2003) High $^{3}He/^{4}He$ ratios in picritic basalts from Baffin Island and the role of a mixed reservoir in mantle plumes. *Nature* 424, 57.

Sumino, H., Kaneoka, I., Matsufuji, K., Sobolev, A.V. (2006) Deep mantle origin of kimberlite magmas revealed by neon isotopes. *Geophysical Research Letters* 33, L16318, doi: 10.1029/2006GL027144.